

Penetrability of asymmetric tunnel microjunction and quasiclassical theory of the scanning tunnel microscope

M. Yu. Sumetskii

Leningrad Electrotechnical Institute of Communications

(Submitted 30 July 1987)

Zh. Eksp. Teor. Fiz. **94**, 7–22 (March 1988)

A semiclassical theory of the penetrability of asymmetric tunnel microjunctions is developed in the one-electron approximation. A general expression is obtained for the penetrability of an asymmetric potential barrier that simulates a microjunction. Various particular cases are investigated, viz., a barrier with rectangular profile, one with a slope that depends on only one coordinate, and one with axial symmetry. Explicit analytic expressions for the transparency, obtained in the free-electron approximation, are used to consider a simple method of reconstructing the surface of a metallic sample from its image obtained with the aid of a scanning tunnel microscope (STM). The influence of localized electron states in the region ahead of the barrier on the penetrability of the microjunction and on the STM image is investigated. The result is compared with the free-electron approximation. An expression is obtained for the penetrability in the presence of the sample of a point defect close to its surface. It is shown that interference phenomena are possible in this case. The location of the tip above the defect can correspond both to a dipole maximum and to a minimum of the transparency. Also considered is emission of electrons from a two-dimensional localized state (quantum well) located on the ground transverse quantum level.

INTRODUCTION

The development of the scanning tunnel microscope (STM) by Binnig and Rohrer¹ has renewed the interest in the penetrability of three-dimensional asymmetric microjunctions having generally speaking an arbitrary shape.^{2–8} Calculations^{2–8} have shown that in many cases the angle between the electron-tunneling direction and the normal to the surfaces of the STM tip and of the investigated sample is small, and the electron beam in the below-barrier region can be regarded as localized near the most probable tunneling path (MPTP).

Good microscope resolution can be obtained just when the width of the tube in which the current is localized is less than the characteristic curvature radius of the investigated surface. This condition, which is equivalent as a rule to the existence of an MPTP, states that the surface must be semiclassical and large-scale. It is the main premise of the present paper.

The theory of penetrability of multidimensional asymmetric potential barriers, based on the existence of an MPTP, was founded in the papers of Kapur and Peierls,⁹ and of Banks, Bender, and Wu.¹⁰ It was further developed in Refs. 11–13. It will be shown below that the methods of this theory lead to significant progress towards the derivation of analytic expressions for the transparency of asymmetric tunnel microjunctions.

We start with the single-particle approximation for electrons and assume that the potential in the below-barrier region is semiclassical and executes an abrupt jump on the surface, as shown in Fig. 1 below. We consider also the possibility of existence of caustics in lieu of the potential jumps.

The value of the current flowing through a microjunction is governed by two interrelated factors: the shape of the potential barrier near the MPTP and the density of the incident electron. In Sec. 2 of this paper we consider the effect of the barrier shape on its penetrability under the assumption

that the electrons outside the barrier are free. The questions considered in Sec. 3 are related to allowance for the possible localization of the electron wave function near the surface outside the barriers.

The first chapter of the paper is devoted to derivation of a general equation for the penetrability of an asymmetric barrier. The explicit analytic equations derived in Chap. 2 are subject to additional assumptions concerning the form of the potential surface in the region below the barrier. It is assumed that the MPTP is a straight line, as is always the case for a rectangular potential barrier, and is valid in a number of other important cases.

Numerical experiments performed in the free-electron approximation by Garcia, Ocal, and Flores² for a potential barrier with a rectangular profile, have yielded a simple semi-empirical dependence of the transparency on the curvature radii of the surfaces and on the points of their intersection with the MPTP. The equally simple and quite rigorous analytic expressions obtained in Chaps. 2 and 3 for the transparency indicate a limited validity of the results of Ref. 3. The expressions obtained in Sec. 2.4 are used to analyze a simple method of reconstructing the surface of the investigated solid from its image obtained by STM. To this end it is possible to neglect, in the zeroth approximation, the pre-exponential factor in the expression for the barrier penetrability, and to consider only the increase of the action along the MPTP. Allowance for the pre-exponential factor will be shown to increase the slopes of the surface outlines or, in other words, to make the image sharper.

If it is assumed that the emission from the STM tip comes mainly from one atom, the natural mode for the tip is that of a localized state.^{2,4} Tersoff and Hamman² proposed for the tip a spherically-symmetric *s*-state model. This model is refined in Chap. 3 on the basis of the theory of resonant tunneling of electrons.¹⁴ The penetrability of an asymmetric barrier is obtained within the framework of this theory. The result is compared with the free-electron approximation.

This is followed by a determination of the influence exerted on the penetrability by a point defect located in the region ahead of the barrier. It is shown that interference phenomena are possible in this case. We investigate also the behavior of the penetrability in the presence of a two-dimensional localized electron state in the sample.

1. MATRIX OF TUNNEL TRANSITIONS

We obtain in this chapter a general expression for the operator of tunneling through a barrier, in a plane-wave basis. If the wave functions of the STM tip and of the sample have a more complicated structure, they can always be expanded, in close vicinities of the points s_1 and s_2 (Fig. 1), in terms of a set of plane waves, and the corresponding transition amplitudes are easily expressed in terms of the transition amplitude for plane waves. The designations "STM tip" and "sample" for regions I and III of Fig. 1 respectively are arbitrary and it will be occasionally convenient later to interchange them.

1.1. Most probable tunneling path (MPTP)

Let a wave be incident from the interior of the tip (region I of Fig. 1b) on the tip surface τ_1 , and let this wave, together with the wave reflected after moving through the tip boundary into the subbarrier region, induce a semiclassical wave function that decays exponentially inside the barrier, and hence also a complex action $S = S_1 + iS_2$ that satisfies the Hamilton-Jacobi equation. In the semiclassical approximation and in the absence of additional symmetry, the tunnel current will be concentrated in a narrow tube around the MPTP that connects the tip and sample surfaces. This path can be obtained in the following manner. Drawing in succession the level surfaces (wave fronts) for S_2 in the classically forbidden region, we construct ultimately a surface which is either tangent to the surface of the solid at some point (Fig. 1b), or on which (at a high applied voltage) ∇S_2 first vanishes at some point. We determine the trajectory s drawn from the initial point and perpendicular to each of the constructed planes at the points of intersection with the latter. By varying the initial properties of the incident wave on the equal-energy surface, we obtain a family of such trajectories. The one on which the integral $\int |\nabla S_2| ds$ is a minimum is in fact the MPTP. We assume that the main contribution to the current is made by electrons incident on the surface at

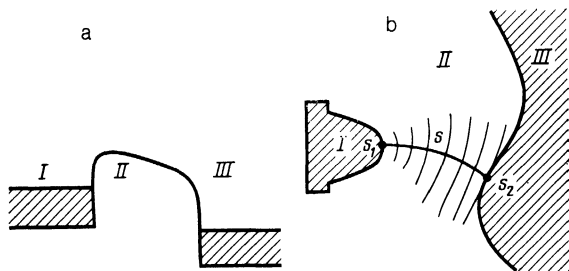


FIG. 1. a) Section through potential relief of STM of the "tip" (I)—vacuum, (II)—sample surface, (III)—structure. b) Illustration of the construction of the MPTP. The arcs represent the wave fronts of the imaginary part of the action S_2 . The curve perpendicular to them, joining the regions I and II, is the MPTP for a suitably chosen boundary condition.

an angle close to the direction of the MPTP. To find the MPTP in the classically forbidden region II we can then put $S_1 = 0$ and substitute the boundary condition $S_2|_{\tau_2} = 0$ for the imaginary part of the action. In this case the action S_2 satisfies the Hamilton-Jacobi equation and the MPTP is a complex classical trajectory. It can be shown that this path is independent of the boundary from which its construction was initiated.

1.2. Semiclassical solution of the Schrödinger equation in the vicinity of the MPTP

We use the fact that in the semiclassical approximation the decisive contribution to the barrier penetrability is made by the wave function in the vicinity s of the MPTP. We define, following Ref. 15, in the vicinity of the path s an orthogonal reference frame, x_1, x_2 , in which the radius vector $\mathbf{r}(M)$ of the point M is of the form $\mathbf{r}(M) = \mathbf{r}(s) + x_1 \mathbf{e}_1(s) + x_2 \mathbf{e}_2(s)$, and the unit vectors $\mathbf{e}_1(s)$ and $\mathbf{e}_2(s)$ are obtained from the principal normal $\mathbf{n}(s)$ and the binormal $\mathbf{b}(s)$ to the MPTP at the point s by rotation through an angle $\vartheta(s)$:

$$\begin{aligned} \mathbf{e}_1 &= \mathbf{n} \cos \vartheta - \mathbf{b} \sin \vartheta, & \vartheta(s) &= \vartheta(s_1) + \int_{s_1}^s T(s) ds. \\ \mathbf{e}_2 &= \mathbf{n} \sin \vartheta + \mathbf{b} \cos \vartheta, \end{aligned} \quad (1.1)$$

Here $T(s)$ is the torsion of the MPTP.

In accordance with the foregoing, the path s is perpendicular to the surfaces τ_1 and τ_2 at the intersection points s_1 and s_2 (Fig. 1b). The equation for the surface τ_j in a small vicinity of the point s_j is therefore

$$s = s_j + \sum_{m,n=1}^2 \Omega_{mn}^{(j)} x_m x_n = s_j + (\Omega_j \mathbf{x}, \mathbf{x}), \quad (1.2)$$

where \mathbf{x} is a two-dimensional vector and $\Omega_j = \|\Omega_{mn}^{(j)}\|$ is a symmetric matrix.

Let the potential $V(\mathbf{r})$ have a semiclassical behavior in the subbarrier region outside the boundaries τ_1 and τ_2 . We are interested only in those solutions of the Schrödinger equation¹⁾

$${}^{1/2} \Delta \Psi + [E - V(\mathbf{r})] \Psi = 0, \quad (1.3)$$

which are localized near the MPTP and have transverse momenta that are small compared with the longitudinal one. It is known^{16,13} then that Eq. (1.3) has in the MPTP vicinity the following semiclassical solution:

$$\begin{aligned} \Psi^\pm(\mathbf{c}, \mathbf{r}) &= [p \det Q(s)]^{-1/2} \\ &\times \exp \left\{ \pm i \int_{s_1}^s ds \left[p - \frac{1}{2p} (Q^{-1}(s) \mathbf{c}, Q^{-1}(s) \mathbf{c}) \right] \right. \\ &\left. + i (Q^{-1}(s) \mathbf{c}, \mathbf{x}) \pm \frac{ip}{2} (Q_s(s) Q^{-1}(s) \mathbf{x}, \mathbf{x}) \right\}. \end{aligned} \quad (1.4)$$

Here \mathbf{c} is a two-dimensional vector with arbitrary constants,

$$p(s) = [2(E - V(0, 0, s))]^{1/2} \quad (1.5)$$

(it is assumed that in the classically forbidden region

$p = i|p|$), and the matrix function $\mathbf{Q}(s)$ satisfies the linear homogeneous differential equation

$$p^2 \mathbf{Q}_{ss} + p p_s \mathbf{Q}_s + \mathbf{F} \mathbf{Q} = 0, \quad \mathbf{F}(s) = \left\| \frac{\partial^2 V}{\partial x_j \partial x_k} \right\|_{\mathbf{r}=(0,0,s)} \quad (1.6)$$

1.3. Tunneling operator in a plane-wave basis

Let a wave be incident at a small angle in region I on the boundary τ_1 and let the wave take in a small vicinity of the point s_1 the form of a plane wave normalized to a unit flux density:

$$\Psi_{I^+} = (p_1^-)^{-1/2} \exp \left\{ i \left[p_1^- - \frac{|p_0|^2}{2p_1^-} \right] (s-s_1) + i p_0 x \right\}. \quad (1.7)$$

The modulus of the momentum $p(s)$ at the potential discontinuities is designated here by

$$p_j^\pm = \lim_{s \rightarrow s_j, \pm 0} |p(s)|. \quad (1.8)$$

The wave function in region I should be a sum of an incident wave and a reflected one: $\Psi_I = \Psi_{I^+} + \Psi_{I^-}$. The reflected wave Ψ_{I^-} can be sought in the form $A \Psi^-(\mathbf{c}, \mathbf{r})$, and the corresponding wave function Ψ_{II^+} in the subbarrier region, which decreases with increasing distance from s_1 , can be designated $B \Psi^+(\mathbf{c}', \mathbf{r})$. We join together the asymptotes Ψ_I and Ψ_{II^+} by equating, in the quasiclassical approximation, these functions and their derivatives on the boundary τ_1 . As a result we get

$$\Psi_{II^+} = \frac{2(p_1^+ p_1^-)^{1/2}}{p_1^- + i p_1^+} \Psi^+(\mathbf{p}_0, \mathbf{r}), \quad (1.9)$$

where the matrix function $\mathbf{Q}(s)$ is uniquely determined by Eq. (1.6) together with the boundary condition

$$\mathbf{Q}(s_1) = \mathbf{E} = \begin{pmatrix} 1 & 0 \\ 0 & 1 \end{pmatrix}, \quad \mathbf{Q}_s(s_1) = -2 \left(1 + \frac{i p_1^-}{p_1^+} \right) \Omega_1. \quad (1.10)$$

In region III, in a small vicinity of s_2 , we represent the outgoing wave in the form

$$\Psi_{III^+} = 2\pi (p_2^+)^{-1/2} \int d\mathbf{p}' T(\mathbf{p}_0, \mathbf{p}') \times \exp \left\{ i \left[p_2^+ - \frac{|p'|^2}{2p_2^+} \right] (s-s_2) + i p' x \right\}. \quad (1.11)$$

To find Ψ_{III^+} it suffices now to match similarly the sums $\Psi_{II^+} + \tilde{A} \Psi^-(\mathbf{c}, \mathbf{r})$ and Ψ_{III^+} on the boundary τ_2 . Here $\tilde{A} \Psi$ is a solution that increases in the direction of s and is exponentially small near τ_1 . As a result we get

$$T(\mathbf{p}_0, \mathbf{p}') = \lambda_1 \lambda_2 (\det \Xi)^{-1/2} \times \exp \left\{ - \int_{s_1}^{s_2} |p| ds - \frac{1}{2} \left(\int_{s_1}^{s_2} \frac{ds}{|p|} \mathbf{Q}^{-2} \mathbf{p}_0, \mathbf{p}_0 \right) - \frac{1}{2} (\Xi \mathbf{Q}^{-1}(s_2) \mathbf{p}_0 - \mathbf{p}', \mathbf{p}_0 - \mathbf{Q}(s_2) \mathbf{p}') \right\}, \quad (1.12)$$

where we use the notation

$$\lambda_j = \frac{2(p_j^- p_j^+)^{1/2}}{p_j^- - i(-1)^j p_j^+}, \quad \Xi = p_2^- \mathbf{Q}_s(s_2) + 2(p_2^- + i p_2^+) \Omega_2 \mathbf{Q}(s_2). \quad (1.13)$$

The expression obtained is valid only under the condition that the matrix $\text{Re } \Xi$ remains positive-definite.

Note that if the boundary τ_j were to correspond not to an abrupt discontinuity of the potential $V(\mathbf{r})$ but to a caustic [in this case $p(s_j) = 0$], it could be shown that Eq. (1.12) remains valid if one puts

$$\lambda_j = 1, \quad \Omega_j = 0. \quad (1.14)$$

Thus, after finding the MPTP and solving the linear matrix equation (1.6) with the boundary condition (1.10), Eq. (1.12) is the solution of the problem of calculating the tunneling matrix.

2. PENETRABILITY OF ASYMMETRIC TUNNEL MICROJUNCTION IN THE FREE-ELECTRON APPROXIMATION

If the potential $V(\mathbf{r})$ outside the barrier is nonreflecting (semiclassical), the current through the microjunction can be obtained in analogy with Ref. 17, in the free-electron approximation, from the equation

$$j = \frac{1}{\pi} \int dE [f(E) - f(E+U)] D(E), \quad (2.1)$$

where f is the electron Fermi distribution function and U is the applied voltage. At low temperature and small U this expression takes the form [$f(E) = \theta(E_f - E)$]

$$j = UD(E_f)/\pi. \quad (2.2)$$

The penetrability $D(E)$ in (2.1) and (2.2) is defined as

$$D(E) = \frac{1}{(2\pi)^2} \int d\mathbf{x} d\mathbf{p}_0 p_2^+ |\Psi_{III^+}|^2 = \frac{1}{(2\pi)^2} \int d\mathbf{p}_0 d\mathbf{p}' |T(\mathbf{p}_0, \mathbf{p}')|^2. \quad (2.3)$$

Substituting (1.12) in (2.3) we get

$$D(E) = \frac{1}{4} |\lambda_1 \lambda_2|^2 (\det \Lambda)^{-1/2} \exp \left(-2 \int_{s_1}^{s_2} |p| ds \right), \quad \Lambda = p_2^- [\mathbf{Q}_s(s_2) + 2\Omega_2 \mathbf{Q}(s_2)] \left(\int_{s_1}^{s_2} \frac{ds}{|p|} \mathbf{Q}^{-2} \right) \mathbf{Q}(s_2). \quad (2.4)$$

The matrix $\mathbf{Q}(x)$ can be regarded here as real and as satisfying the equation (1.6) with the boundary condition

$$\mathbf{Q}(s_1) = \mathbf{E}, \quad \mathbf{Q}_s(s_1) = -2\Omega_1. \quad (2.5)$$

The barrier penetrability, as expected, does not depend on the behavior of the potential in the classically allowed region. Expression (2.4) is the product of a pre-exponential factor and an exponentially growing action along the MPTP. The pre-exponential factor accounts for the geometric singularities of the surface and of the potential as a whole. The condition that it vanish at infinity determines the boundary of the region in which the considered complex classical trajectory is indeed the MPTP and in which the employed ap-

proximation is valid. This region, in which the matrix $\mathbf{Q}_s(s_2)\mathbf{Q}^{-1}(s_2) + 2\mathbf{\Omega}_2$ is positive-definite, can be naturally called the region of tunneling stability of the path s , in analogy with the concept of the stability of the trajectories corresponding to classically allowed motion.¹⁵

We consider in the present chapter the simplest forms of a potential barrier. The potential below the barrier will be regarded in Sec. 2.1 as independent of the coordinates, in 2.2 as dependent on one of the coordinates, and in 2.3 as having axial symmetry. In Sec. 2.4 we consider a simple method of reconstituting the sample surface from its image with the aid of STM.

2.1. Potential barrier with rectangular profile

In this model, used in many papers,²⁻⁸ the image forces are neglected and it is assumed that the slope of the potential barrier is small. The latter condition is met, for example, if the tip and sample have equal work functions at low applied voltage.

In this case the MPTP is the shortest linear segment joining the surfaces τ_1 and τ_2 . Since the potential in the sub-barrier region is independent of the coordinates, we have $p(s) \equiv p_1^+$ and $F(s) \equiv 0$. The solution of Eq. (1.6) is therefore a matrix linear in s . With allowance for the boundary condition (2.5), we get

$$\mathbf{Q}(s) = \mathbf{E} - 2\mathbf{\Omega}_1(s - s_1). \quad (2.6)$$

The integral in Eq. (2.4) for Λ can be easily calculated and the expression for the penetration takes the form

$$D(E) = \frac{|\lambda_1\lambda_2|^2 \exp(-2p_1^+d)}{8d \det^{1/2}(\mathbf{\Omega}_1 - \mathbf{\Omega}_2 + 2d\mathbf{\Omega}_2\mathbf{\Omega}_1)}, \quad (2.7)$$

where d is the MPTP length. The determinant in the denominator of (2.7) can be easily verified to be invariant to interchange of the matrices $\mathbf{\Omega}_1$ and $\mathbf{\Omega}_2$, which are generally noncommutative.

Assume that the misalignment of the principal axes of the surfaces τ_1 and τ_2 is small and that the matrices $\mathbf{\Omega}_1$ and $\mathbf{\Omega}_2$ can be regarded as simultaneously diagonal. We introduce the principal curvature radii of the surface τ_j at the point s_j :

$$R_k^{(j)} = (-1)^j (2\mathbf{\Omega}_{kk}^{(j)})^{-1}. \quad (2.8)$$

Recognizing that $\mathbf{\Omega}_{kl}^{(j)} = 0$ if $k \neq l$, we get

$$D(E) = \frac{|\lambda_1\lambda_2|^2 (R_1^{(1)}R_1^{(2)}R_2^{(1)}R_2^{(2)})^{1/2} \exp(-2p_1^+d)}{4d (R_1^{(1)} + R_1^{(2)} + d)^{1/2} (R_2^{(1)} + R_2^{(2)} + d)^{1/2}}. \quad (2.9)$$

Equation (2.9) is always valid, for example, for a spherical tip, for which the matrix $\mathbf{\Omega}_1$ is diagonal in any orthogonal coordinate frame. It is therefore always possible to choose the unit vectors \mathbf{e}_1 and \mathbf{e}_2 for which the matrix $\mathbf{\Omega}_2$ is also diagonal.

Equations (2.7) and (2.9) solve in the semiclassical approximation the problem posed in Ref. 3. The singularity of (2.7) or (2.9) as $d \rightarrow 0$ is due to the fact that at $p_1^+d \lesssim 1$ the penetrability begins to receive contributions from incident waves having large transverse momenta \mathbf{p}_0 and for which the method employed is no longer valid. In Sec. 3.1 below, in which the results are compared with Ref. 3 in greater detail,

it is shown that this divergence is eliminated in the approximation in which the tip is in a localized state.

2.2. Allowance for change of potential in the sub-barrier region in the $\mathbf{F} \equiv 0$ approximation

If $d \ll R_k^{(j)}$, the MPTP is close, independently of the slope of the potential barrier, to the shortest linear segment joining the surfaces τ_1 and τ_2 . In this case the inhomogeneity of the potential in the direction transverse to the MPTP is small and we can put $\mathbf{F} = 0$. The value of \mathbf{F} can be neglected also in some other cases (e.g., in the case considered in preceding section). The solution of Eq. (1.6) takes now the form

$$\mathbf{Q}(s) = \mathbf{E} - 2p_1^+ \int_{s_1}^s \frac{ds}{|p|} \mathbf{\Omega}_1, \quad (2.10)$$

and for the penetrability we obtain the equation

$$D(E) = \frac{|\lambda_1\lambda_2|^2 \exp\left(-2 \int_{s_1}^{s_2} |p| ds\right)}{8\tau \det^{1/2}(p_1^+\mathbf{\Omega}_1 - p_2^-\mathbf{\Omega}_2 + 2p_1^+p_2^-\tau\mathbf{\Omega}_2\mathbf{\Omega}_1)},$$

$$\tau = \int_{s_1}^{s_2} \frac{ds}{|p|}. \quad (2.11)$$

This result is somewhat more complicated than (2.7) and allows us to take the slope of the potential barrier into account. Let the applied voltage be so high that the barrier is close to triangular (Fig. 2) and the point s_2 is a simple turning point. In the simplest case, putting $V(0,0,s) = -(s - s_1)U/d$, as well $\mathbf{\Omega}_2 = 0$ and $\lambda_2 = 1$ in accordance with (1.14), we get

$$D(E) = \frac{|\lambda_1|^2 U}{4(p_1^+)^2 d} (R_1^{(1)}R_2^{(1)})^{1/2} \exp\left[-\frac{2(p_1^+)^2 d}{3U}\right]. \quad (2.12)$$

This expression is valid if the ratio $(p_1^+)^2/2U$ is less than unity and much less than $R_k^{(1)}/d$. It makes it possible, together with Eq. (2.1), to determine in principle the average radius of the surface $(R_1^{(1)}R_2^{(1)})^{1/2}$ from the current-voltage characteristic $j(U)$ [see also Eq. (3.9)]. The potential of the image forces can similarly be taken into account in the framework of the above approximation.

2.3. Potential barrier with axial symmetry

If the characteristic curvature radii of the surface are of the same order as the barrier width, and the barrier profile is at the same time far from rectangular, the approximations of the preceding sections are incorrect. The MPTP, however, can turn out to be linear also in a more general case. Thus, if the STM tip is spherical, it can be assumed with good accuracy that the MPTP is part of a perpendicular line drawn from the center of the tip to the surface of the sample, and the

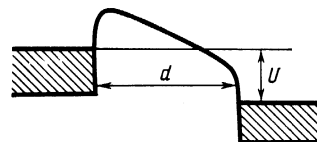


FIG. 2. Profile of potential surface with high applied voltage.

symmetry of the potential near the MPTP is the same as the symmetry of the surface τ_2 . In this approximation one can choose a basis in which Ω_1 , Ω_2 , and F are diagonal simultaneously, and Eq. (1.6) splits into two independent differential equations:

$$p^2 q_{ss}^{(j)} + p p_s q_s^{(j)} + f^{(j)} q = 0, \quad Q = \begin{pmatrix} q^{(1)} & 0 \\ 0 & q^{(2)} \end{pmatrix}, \quad F = \begin{pmatrix} f^{(1)} & 0 \\ 0 & f^{(2)} \end{pmatrix} \quad (2.13)$$

with boundary conditions

$$q^{(j)}(s_1) = 1, \quad q_s^{(j)}(s_1) = -2\Omega_{jj}^{(j)} = (R_j^{-1})^{-1}.$$

It is convenient to introduce matrices t_j that depend only on the potential inside the barrier and are not connected formally with the forms of the surfaces τ_1 and τ_2 . To this end, we determine the solutions $q_{mn}^{(j)}$ of Eq. (2.13) with the boundary conditions

$$q_{1n}^{(j)}(s) \underset{s \rightarrow s_{1n}}{\approx} 1, \quad q_{2n}^{(j)}(s) \underset{s \rightarrow s_{1n}}{\approx} \int_{s_{1n}}^s \frac{ds}{|p|}. \quad (2.14)$$

Each of the solutions $q_{m1}^{(j)}$ can be represented as a linear combination of solutions $q_{m2}^{(j)}$, and the coefficients of the combination determine in fact the matrix elements t_j :

$$q_{m1}^{(j)}(s) = t_{m1}^{(j)} q_{12}^{(j)}(s) + t_{m2}^{(j)} q_{22}^{(j)}(s), \quad t_j = \|t_{mn}^{(j)}\|. \quad (2.15)$$

Equation (2.4) for the penetrability takes, in the notation introduced, the form

$$D(E) = \frac{|\lambda_1 \lambda_2|^2}{4(\Lambda_{11} \Lambda_{22})^{1/2}} \exp\left(-2 \int_{s_1}^{s_2} |p| ds\right),$$

$$\Lambda_{jj} = t_{21}^{(j)} (t_{12}^{(j)}) - 2p_1^+ \Omega_{jj}^{(1)} t_{22}^{(j)} + 2p_2^- \Omega_{jj}^{(2)} t_{11}^{(j)} - 4p_1^+ p_2^- \Omega_{jj}^{(1)} \Omega_{jj}^{(2)} t_{21}^{(j)}.$$

(2.16)

If the MPTP is a symmetry axis of infinite order, then $t_1 = t_2$ and $\Omega_{11}^{(k)} = \Omega_{22}^{(k)}$. For $\lambda_j = 1$ and $\Omega_{jj}^{(k)} = 0$ Eq. (2.16) coincides then with expression (10) of Ref. 18, averaged over the transverse momenta.²⁾

Equation (2.16) and elementary numerical methods yield the penetrability of barriers with potential reliefs of quite general form, such as obtained, e.g., for certain surface models in Refs. 19 and 20. Note that Eq. (2.13) can always be solved analytically if the variables of the potential $V(\mathbf{r})$ in the sub-barrier region can be separated. Incidentally, an analytic solution can be obtained in this case also for the matrix equation (1.6).

2.4. The theory of the STM image

The trajectory of the STM tip, which traces the dc current level, depicts the surface of a solid with inevitable distortions that depend on the distance from the tip to the surface, and on the forms and internal structures of the tip and the sample. In the simplest case of an ideal metal, the theory of the STM image can be based on the calculations of the present chapter, i.e., in the free-electron approximation. This approximation may be useful also in a more general case of, say, investigations of solid-surface microroughnesses (microprojections or micropits) with typical dimen-

sions 1–10 nm.^{21,22} The surface of a sample can be readily determined by method of the present section from its STM image. A particular case of the approach presented, based on the results of Ref. 3, is contained in Ref. 23.

We assume for simplicity that the barrier is rectangular, as in Sec. 2.1. In the exponential approximation, the condition that the current (2.1) be constant is then equivalent that the length of the linear MPTP be constant. This length, just as the tip radius, can be approximately calculated from the given current and from the work function.² Assume that we know the surface traced by the STM tip and the shape of the tip (the experimental determination of the tip shape is the subject of Ref. 22). We can then construct also the envelope the family of tip surfaces traced by the moving tip. The sought surface of the solid is none other than the geometric locus of the end points of the MPTP determined from each point of the envelope. It is shown in Fig. 3 by the dashed line $A'B'$.

The condition that the current be constant (at constant U) can be found more accurately, with allowance for the pre-exponential factor, by substituting Eq. (2.9) [or (2.7)] in (2.1):

$$d + \Delta d = \text{const},$$

$$\Delta d = \frac{1}{4p_1^+} \ln \left[d^2 \left(\frac{1}{R_1^{(1)}} + \frac{1}{R_1^{(2)}} + \frac{d}{R_1^{(1)} R_1^{(2)}} \right) \times \left(\frac{1}{R_2^{(1)}} + \frac{1}{R_2^{(2)}} + \frac{d}{R_2^{(1)} R_2^{(2)}} \right) \right]. \quad (2.17)$$

This formula is valid only when Δd is smaller than d . Therefore allowance for the pre-exponential factor makes it possible only to correct the results of the exponential approximation. A typical result of the correction is shown in Fig. 3 (the solid curve AB). It was obtained by increasing the lengths d of each MPTP reconstructed from the envelope of the family of tip surfaces, by an amount Δd . It can be seen that allowance for the pre-exponential factor makes it possible to make the surface outline more contrasty. The reason is that the current-beam width that determines the pre-exponential factor, and hence also the value of the current, is larger near a concave surface than near a convex one.

Note that the expression obtained in the next chapter for the penetrability of the potential barrier in the approximation of a localized state for the tip make it possible to

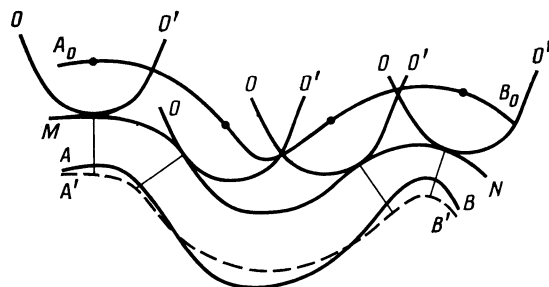


FIG. 3. Reconstruction of the surface of a metallic sample from the STM image. A_0B_0 —STM trace, OO' —STM tip surface, MN —envelope of the family of tip surfaces, $A'B'$ —sample surface reconstructed in the exponential approximation, AB —sample surface reconstructed with allowance for the pre-exponential factor.

refine Eq. (2.17). It is necessary to use Eq. (3.8) in lieu of (2.9).

3. INFLUENCE OF STATES LOCALIZED OUTSIDE THE BARRIER ON THE MICROJUNCTION PENETRABILITY

The correct electron wave function of a solid, near the point s_j , is a linear combination of plane waves:

$$\Psi_{\mathbf{q}}(\mathbf{r}) = \int_{|\mathbf{p}|^2=2E} d\mathbf{p} C(\mathbf{q}, \mathbf{p}) e^{i\mathbf{p}\mathbf{r}} \quad (3.1)$$

[$C(\mathbf{q}, \mathbf{p}) \sim \delta(\mathbf{q} - \mathbf{p})$ for $p_z > 0$ in the free-electron approximation]. In the problems considered in the present chapter it is assumed that the free-electron approximation remains valid only at the exit from below the barrier. In Sec. 3.1 we discuss the localized-states model for the tip, and obtain the penetrability of the potential barrier in this model. In Sec. 3.2 is considered the case when a point defect is present in the subsurface of the sample. In Sec. 3.3 we obtain an expression for the penetrability for electron emission from a two-dimensional localized state (quantum well). The penetrability $D(E)$ is defined for all the considered structures in such a way that the equations (2.1) and (2.2) for the current remain in force.

3.1. Model of localized state for the tip

In Refs. 2 and 4, in contrast to Ref. 3, the tunnel current is defined as the current from the bound state of the tip atom closest to the sample. This model was investigated in Ref. 7 in the self-consistent field approximation. It can be treated more lucidly by using the model with resonant tunneling of electrons through a bound state.^{24,25,14}

Let a bound state simulating the tip be located in the sub-barrier region near the surface τ_1 (Fig. 4a). We assume that the free-electron approximation is valid in regions I and III. The resonant penetrability of the potential barrier can then be represented in the Breit-Wigner approximation by the equation¹⁴

$$D(E) = \frac{1/2 \Gamma_+ \Gamma_-}{(E - E_0)^2 + 1/4 (\Gamma_+ + \Gamma_-)^2}. \quad (3.2)$$

Here E_0 is the bound-state level of surface atom, while Γ_+ and Γ_- are the probabilities of the decay of this state in the sample and in the tip, respectively. We shall assume that $\Gamma_- \gg \Gamma_+$, i.e., that the integral of the atom electron wave function overlap with the tip states is substantially larger than with the sample states. This is always the case if the barrier is wide enough. If we assume furthermore that the temperature and the applied voltage are low, so that the energy interval ΔE of the electrons contributing to the current, just as $|E - E_0|$, is smaller than Γ_- , we can put

$$D(E) = \frac{2\Gamma_-}{4(E - E_0)^2 + \Gamma_-^2} \Gamma_+ \approx 2\Gamma_+ / \Gamma_-. \quad (3.3)$$

Numerical calculations show⁷ that for real atoms these equations are of correct order of magnitude. Assume that the wave function of the tip is an s wave specified in a spherically symmetric square potential well of radius R , whose outer boundary coincides with τ_1 . This wave function, normalized in a sphere of radius R , takes in the sub-barrier region the form

$$\Psi_s(\mathbf{r}) = 2p_1^- \exp[-p_1^+(r-R)] / (2\pi R)^{3/2} (p_1^- + ip_1^+) r \quad (3.4)$$

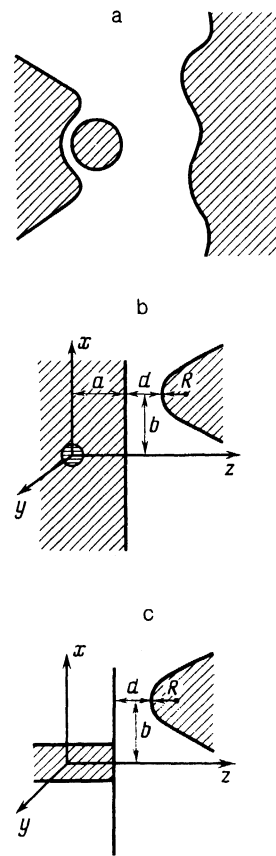


FIG. 4. a—Illustrating the calculation of the penetrability in the localized-state approximation for the tip; b—point defect near the sample surface; c—two-dimensional localized state (quantum well) in sample.

(the origin is at the center of the sphere). Since the form of the atom bound-state wave function is in fact unknown, this expression is valid for a real atom apart from a factor on the order of unity.² It is now easy to show that the wave function (3.4) will match the solution (1.4), which is of the form

$$\frac{(p_1^-)^{1/2} \lambda_1}{(2\pi R)^{3/2}} \Psi_+(0, \mathbf{r}), \quad (3.5)$$

if the matrix $\mathbf{Q}(s)$ for it is defined by the boundary conditions

$$\mathbf{Q}(s_1) = R\mathbf{E}, \quad \mathbf{Q}_s(s_1) = \mathbf{E}. \quad (3.6)$$

The quantity Γ_- is of the order of the atom level spacing. For low-lying states we have $E_0 \sim R^{-2}$, and we can therefore put $\Gamma_- = \pi^2 \kappa^{-1} R^{-2}$, $\kappa \sim 1$. As a result, in analogy with the preceding chapter, we get

$$D(E) = \kappa |\lambda_1 \lambda_2|^2 p_1^- R \exp(-2 \int_{s_1}^{s_2} |p| ds) / p_2^- \det^{1/2} \mathbf{Q}(s_2) \det^{1/2} [\mathbf{Q}_s(s_2) + 2\mathbf{\Omega}_2 \mathbf{Q}(s_2)]. \quad (3.7)$$

We get hence for a barrier with rectangular profile

$$D(E) = \kappa |\lambda_1 \lambda_2|^2 p_1^- R (R_2^{(1)} R_2^{(2)})^{1/2} \exp(-2p_1^+ d) / 4 p_1^+ (d+R) (d+R+R_2^{(1)})^{1/2} (d+R+R_2^{(2)})^{1/2}. \quad (3.8)$$

Comparison of this expression with Eq. (3.9) obtained in the

free-electron approximation shows that at $d \gg R$ they differ only by a factor of order unity. In the opposite case of small d Eq. (3.8), in contrast to (3.9) has no singularity. The quantity R in (3.8) is of the order of the characteristic reciprocal momentum. The singularity with respect to d in (2.9) can, in accord with the remark following this equation, be smoothed by adding to d a quantity of the order of $(p_1^+)^{-1}$. At $d \ll R_k^{(j)}$ the penetrability (2.9), just as (3.8), turns out to be proportional to the effective radius of curvature:

$$R_{\text{eff}} = \left[\left(\frac{1}{R_1^{(1)}} + \frac{1}{R_2^{(1)}} \right) \left(\frac{1}{R_1^{(2)}} + \frac{1}{R_2^{(2)}} \right) \right]^{-1/2},$$

in full accord with the guess made by the authors of Ref. 3. A comparison of expressions (2.9) and (3.8) with the semi-empirical formula of Ref. 3 for the penetrability shows, however, that the latter cannot be valid if $R_k^{(j)}$ and d are of the same order.

In the localized state approximation for a tip, in analogy with the preceding chapter, it is easy to consider also potential barriers of other forms. Thus, for a tip in a strong electric field (Fig. 2) we now obtain in lieu of (2.12)

$$D(E) = \frac{\kappa |\lambda_1 \lambda_2|^2 p_1^- R}{p_1^+ [R + d(p_1^+)^2/U]} \exp \left[-\frac{2(p_1^+)^3 d}{3U} \right], \quad (3.9)$$

from which we see that in contrast to (2.12), in a very strong field $U \gg (p_1^+)^2 d/R$ the penetrability ceases to depend on R , and in the opposite case $U \ll (p_1^+)^2 d/R$ this result coincides with the free-electron approximation. Under more general assumptions, Γ_+ was calculated for axisymmetric potentials in Refs. 12.

3.2. Point defect in the region ahead of the barrier

Individual point defects in a thin insulator film were revealed in Ref. 26 by current oscillations produced by successive filling the defects with electrons of a localized bound state and then emptying them. A filled defect is coupled to the electrons by Coulomb repulsion, and an empty one can be approximately simulated by a small-radius potential. In principle, noise from an individual effect can be observed also when the defect is in the sub-barrier region. In the present section we confine ourselves to the case when a small-radius defect is located ahead of the barrier. The problem is to find the extent to which STM can react to an empty neutral defect as a function of the distance from the defect to the sample surface and of other parameters.

Let, for simplicity, the sample surface τ_1 be plane, and let it be close to a point defect (Fig. 4b) which we simulate by a zero-radius potential.²⁷ The wave function in the region ahead of the barrier, where the potential is assumed to be constant everywhere around the defect, can be sought in the form of a sum of incident and reflected waves:

$$\begin{aligned} \Psi(\mathbf{r}) = & (p_z^-)^{-1/2} \left\{ \exp(ip_z^- z + ip_x x + ip_y y) \right. \\ & + \frac{p_z^- - ip_z^+}{p_z^- + ip_z^+} \exp[ip_z^- (2a - z) + ip_x x + ip_y y] \\ & \left. - \frac{\alpha(p_x, p_y)}{p^+ + ip_1^-} \left[\frac{\exp(ip_1^- r)}{r} + \frac{(p_1^- - ip_1^+) \exp(ip_1^- |2\mathbf{a} - \mathbf{r}|)}{(p_1^- + ip_1^+) |2\mathbf{a} - \mathbf{r}|} \right] \right\}, \end{aligned} \quad (3.10)$$

where $(p_z^\pm)^2 = (p_1^\pm)^2 - p_x^2 - p_y^2$, and $(p^*)^2/2$ is the en-

ergy of the bound state of the defect. We have then in accord with the general methods²⁷

$$\alpha(p_x, p_y) = 1 + \frac{p_z^- - ip_z^+}{p_z^- + ip_z^+} \exp(2ip_z^- a). \quad (3.11)$$

In the derivation of (3.10) and (3.11) we have assumed that the distance from the defect to the surface is much larger than the electron wavelength: $p_z^- a \gg 1$. The inverse case is close to the one considered in the preceding section.

Following its continuation through the barrier into region III, the sum of the plane and spherical waves (3.10) turns in the sum of outgoing waves $\Psi_p^+ + \Psi_s^+$ of the form (1.4), the first of which is a continuation of the plane wave and the other of the spherical. Accordingly, the flux at the exit from under the barrier contains three terms:

$$\begin{aligned} D(E) = & \frac{p_z^-}{(2\pi)^2} \int dx dy \int_{|p_x|=p_1^-} dp \{ |\Psi_p^+|^2 + |\Psi_s^+|^2 \\ & + 2 \operatorname{Re}[\Psi_p^+ (\Psi_s^+)^*] \} = D_p + D_s + D_{ps}. \end{aligned} \quad (3.12)$$

Here D_p and D_s are the barrier penetrabilities for plane and spherical waves, respectively, and D_{ps} is an interference term. Assume that the STM tip is spherically symmetric with radius R , and that the barrier profile is rectangular. We obtain then

$$D_p = \frac{|\lambda_1 \lambda_2|^2 R}{4d} \exp(-2p_1^+ d), \quad (3.13)$$

$$D_s = \frac{2|\lambda_1 \lambda_2|^2 p_1^- R}{[(p^*)^2 + (p_1^-)^2] (|\chi|^2 + Rd)} \exp \left(-2p_1^+ d - \frac{p_1^+ db^2}{|\chi|^2 + Rd} \right), \quad (3.14)$$

$$\begin{aligned} D_{ps} = & -\operatorname{Im} \left[\frac{2|\lambda_1 \lambda_2|^2 \alpha(0, 0) (p_1^+)^{3/2} R}{(p^+ + ip_1^-) (p_1^-)^{3/2} v^+} \right. \\ & \left. \times \exp \left(-2p_1^+ d - \frac{p_1^+ v^- b^2}{2\chi v^+} \right) \right], \end{aligned} \quad (3.15)$$

where

$$\chi = d + ia p_1^+ / p_1^-, \quad v^\pm = (2d + R) \chi \pm Rd.$$

Here b is the displacement of the tip relative to the defect in the xy plane. It is taken into account in (3.14) that while the tunneling electrons are mainly those having small transverse momenta directly ahead of the barrier, scattering by the defect causes a contribution to the penetrability to be made by electrons with large initial transverse momenta. The coefficient $\alpha(0, 0)$ in (3.15) can vanish when the defect is located on a plane-wave node with $p_x = p_y = 0$.

Owing to the decrease of the spherical-wave pre-exponential factor which is proportional to the distance to the defect, D_s and D_{ps} are smaller than D_p . It is they, however, which determine the dependence, in which we are interested, of the penetrability on b . Retaining in (3.15) only the explicit dependence on b , we can rewrite this equation in the form

$$D_{ps} = A \cos(\varphi_1) \cos(\varphi_2 + \eta b^2) \exp(-\omega b^2), \quad (3.16)$$

from which it can be seen that with increase of b the penetra-

bility is in general oscillatory. Since $\varphi_2 \neq 0$ in the general case, both a local maximum and a minimum of the penetrability can be reached at $b = 0$ (this interference effect is similar to that noted in Ref. 14).

If the defect lies deep, $a \gg ap_1^-/p_1^+$, we get

$$\begin{aligned} A &= 4|\lambda_1 \lambda_2|^2 (p_1^-)^{3/2} R / [(p_1^-)^2 + (p_1^-)^2]^{1/2} (p_1^+)^{3/2} (2d+R)a, \\ \varphi_1 &= p_1^- a + \arctg(p_1^+/p_1^-), \quad \varphi_2 = \varphi_1 - \arctg(p_1^-/p_1^+), \\ \omega &= 0, \quad \nu_1 = -p_1^-/2a. \end{aligned} \quad (3.17)$$

It turns out then that $D_s \ll D_{ps}$, and the contribution of D_s can be neglected. Equations (3.17) enable us to trace the penetrability oscillations more clearly. It is seen from these equations, in particular, that at $b = 0$ a minimum penetrability, just as a maximum, can be reached. In the opposite limiting case $a \ll dp_1^-/p_1^+$ we have $\eta = 0$ and $\omega = p_1^+ [2(R+d)]^{-1}$, therefore the penetrability always decreases exponentially as a function of b .

In the general case, putting $p_1^+ \sim p_1^- \sim p^* \sim 0.3$ a.u. and $a \sim R \sim d \sim 10 \text{ \AA}$, we obtain $D_s \sim D_{ps} \sim 0.3 D_p$. The first "half-period" of the oscillations in b is then approximately 5 \AA , and the corresponding displacement of the STM tip along the z axis, at $\cos \varphi_1 \sim 0.5$, is of the order of 0.3 \AA .

3.3. Emission of electrons from a quantum well

Assume, as in the preceding section, that the sample surface is plane, the barrier profile rectangular, and the tip spherically symmetric with radius R . Let a two-dimensional localized state of electrons (quantum well) be located in the sample perpendicular to the surface (Fig. 4c). We assume for simplicity the potential in the quantum well to be approximately oscillatory, $V(\mathbf{r}) = \omega_0^2 x^2/2$, and take into account only electrons located on the first transverse quantum level. If the barrier is wide enough, only these electrons make the main contribution to the penetrability.

The incident wave in the quantum well, normalized to a unit flux and to a unit strip along y , is given by

$$\Psi(\mathbf{r}) = \frac{\omega_0^{1/4}}{\pi^{1/4} (p_1^-)^{1/2}} \exp \left[i \left(p_1^- z - \frac{p_1^2 + \omega_0}{2p_1^-} z - \frac{\omega_0 x^2}{2} + ip_y y \right) \right]. \quad (3.18)$$

It is taken into account in (3.18) that the only states considered are those for which the longitudinal momentum p_{1z}^- exceeds substantially the transverse ones p_y and $\omega_0^{1/2}$. Continuing the incident wave (3.18) together with the reflected one through the barrier, we obtain in region III the outgoing wave Ψ_{III}^+ . Calculations lead to the following equation for the penetrability in the considered structure:

$$\begin{aligned} D(E) &= \frac{p_2^+}{2\pi} \int dx dy dp_y |\Psi_{III}^+|^2 \\ &= \frac{(\omega_0 p_1^+)^{1/2}}{2\{d(p_1^+ + \omega_0 d) [p_1^+ + \omega_0(d+R)]\}^{1/2}} \\ &\quad \times \exp \left[-2p_1^+ d - \frac{\omega_0 p_1^+ b^2}{p_1^+ + \omega_0(d+R)} \right], \end{aligned} \quad (3.19)$$

where b is the displacement of the tip relative to the center of the well in the xy plane. Comparing this equation with (3.18) we see that, as expected, the penetrability, and with it the current (2.2), duplicates the density of the electron wave

function of the sample, $D \propto |\Psi(b)|^2$, if R and d are much smaller than the characteristic dimension p_1^+/ω_0 of the localized state. Conversely, in the opposite limit $d \gg p^+/\omega_0$ the dependence of (3.19) on b at $d \gg ap_1^+/p_1^-$ is equal, apart from a constant, to the b dependence of the penetrability of a spherical wave (3.14) from a point defect located close to the surface.

4. CONCLUSION

The quasiclassical approximation in the sub-barrier region, on which the results of the present paper is based, cannot take correctly into account the rapid change of the potential relief over a distance on the order of the electron wavelength. Suffering from the same defect is also the STM, whose image is roughly speaking a smoothed image of a surface of width larger than the electron wavelength. The error of the approximation employed seems therefore frequently to agree with the STM measurement error. Even in this approximation, however, reconstruction of a three-dimensional potential from surfaces described by the STM tip (this should be in the general case a family of surfaces that depend parametrically on the current or on the applied voltage) is a complicated nonlocal inverse problem for the Poisson equation.

We disregarded above effects connected with existence of not one but several MPTP. The current beams in the vicinities of these paths can be independent, but may also intersect. The intersection takes place in the vicinity of the boundary of the region of the MPTP tunnel stability. The bifurcation effects that accompany this phenomenon can be investigated by taking into account in the initial Hamiltonian not only the terms quadratic in the coordinates transverse to the MPTP, but also the terms of higher order. In the general case, however, inclusion of the next-order terms makes for a more accurate expression for the penetrability of the potential barrier.

The use of the employed method is obviously not limited to the examples above. Thus, it is easy to take into account the interference, investigated in Ref. 28, of tunneled electrons reflected (at a sufficiently high applied voltage) from a surface-potential jump. It would be possible to calculate, in addition to Sec. 3.2, the penetrability, in the presence of a Coulomb center, in the region ahead of the barrier. One can determine the images of dislocations and superlattices by simulating them by potential jumps and by small-radius potentials, calculate the penetrability for the charge-density-wave model considered in Ref. 29, etc.

¹The atomic system of units is used throughout.

²In the exponential of Eq. (10) of Ref. 18, a minus sign was left out directly after the square bracket in the numerator, so that the factors contained there in the square brackets cancel out.

³G. Binnig, H. Rohrer, Ch. Gerber, and E. Weibel, Phys. Rev. Lett. **49**, 57 (1982).

⁴J. Tersoff and D. R. Hamann, *ibid.* **50**, 1998 (1983), Phys. Rev. **B31**, 805 (1985).

⁵N. Garcia, C. Ocal, and F. Flores, Phys. Rev. Lett. **50**, 2002 (1983). N. Garcia and N. Flores, Physica **127B+C**, 137 (1984).

⁶A. Baratoff, Physica **127B+C**, 143 (1984).

⁷T. E. Feuchtwang, P. H. Cutler, and N. M. Miskovsky, Phys. Lett. **A99**, 167 (1983).

- ⁶E. Stoll, A. Baratoff, A. Selloni, and P. Carnevali, *J. Phys.* **C17**, 3073 (1984).
- ⁷N. D. Lang, *Phys. Rev. Lett.* **55**, 230 (1985).
- ⁸M. V. Krylov and R. A. Suris, *Zh. Eksp. Teor. Fiz.* **88**, 2204 (1985) [*Sov. Phys. JETP* **61**, 1303 (1985)]. *Poverkhnost'* **10**, 20 (1986).
- ⁹P. L. Kapur and R. Peierls, *Proc. Roy. Soc.* **A163**, 606 (1937).
- ¹⁰T. Banks, C. M. Bender, and T. T. Wu, *Phys. Rev.* **D8**, 3366 (1973). T. Banks and C. M. Bender, *ibid.* **D8**, 3366 (1973) [*Sic!*].
- ¹¹J.-L. Gervais and B. Sakita, *Phys. Rev.* **D16**, 3507 (1977). H. J. De Vega, J.-L. Gervais, and B. Sakita, *Nucl. Phys.* **B139**, 20 (1978).
- ¹²M. Yu. Sumetskii and G. V. Dubrovskii, *Dokl. Akad. Nauk SSR* **245**, 75 (1979). M. Yu. Sumetskii, *Teor. Mat. Fiz.* **45**, 64 (1980). *Zh. Eksp. Teor. Fiz.* **89**, 618 (1985) [*Sov. Phys. JETP* **62**, 355 (1985)].
- ¹³A. Schmid, *Ann. Phys. (N. Y.)* **170**, 333 (1986).
- ¹⁴M. Yu. Sumetskii, *Pis'ma Zh. Eksp. Teor. Fiz.* **44**, 287 (1986) [*JETP Lett.* **44**, 369 (1986)].
- ¹⁵V. M. Babich and V. S. Buldyrev, *Asymptotic Methods in Short-Wave Diffraction Problems* [in Russian], Nauka, 1972.
- ¹⁶V. P. Maslov, *The Complex WKB Method in Nonlinear Equations* [in Russian], Nauka, 1977.
- ¹⁷K. B. Duke, in: *Tunnel Phenomena in Solids*, E. Burstein and S. Lundquist, eds. [Russ. transl.], Mir, 1973, p. 36.
- ¹⁸M. Yu. Sumetskii, *Zh. Tekh. Phys.* **54**, 2227 (1984) [*Sov. Phys. Tech. Phys.* **29**, 1305 (1984)].
- ¹⁹A. A. Lucas, J. P. Vigneron, J. Bono, *et al.*, *J. de Phys. Coll.* **95**, C9-125 (1984).
- ²⁰H. Morawitz, I. P. Batra, R. Reinsh, and G. H. Henry, *Surf. Sci.* **180**, 333 (1987).
- ²¹J. K. Gizewski, A. Humbert, J. G. Bendarz, and B. Reihl, *Phys. Rev. Lett.* **55**, 951 (1985).
- ²²G. F. A. Van de Walle, H. Van Kempen, and P. Wyder, *Surf. Sci.* **167**, L219 (1986).
- ²³R. Chicon, M. Ortuno, and J. Abellan, *ibid.* **181**, 107 (1987).
- ²⁴A. V. Chaplik and M. V. Entin, *Zh. Eksp. Teor. Fiz.* **67**, 208 (1974) [*Sov. Phys. JETP* **40**, 106 (1975)].
- ²⁵I. M. Lifshitz and V. Ya. Kirpichenkov, *ibid.* **77**, 989 (1979) [*Sov. Phys. JETP* **50**, 499 (1979)].
- ²⁶M. E. Welland and R. H. Koch, *Appl. Phys. Lett.* **48**, 724 (1986).
- ²⁷Yu. N. Demkov and V. N. Ostrovskii, *Method of Zero-Radius Potentials in Atomic Physics* [in Russian], Leningrad Univ. Press, 1975.
- ²⁸R. S. Becker, J. A. Golovchenko, and B. S. Swartzentruber, *Phys. Rev. Lett.* **55**, 987 (1985). G. Binnig, K. H. Frank, H. Fuchs, *et al.*, *ibid.* **55**, 901 (1985).
- ²⁹J. Tersoff, *ibid.* **57**, 440 (1986).

Translated by J. G. Adashko

Editor's note: M. Yu. Sumetskii, "Penetrability of asymmetric tunnel microjunction and quasiclassical theory of the scanning tunnel microscope," *Sov. Phys. JETP* **67** (3), p. 438 was listed in the table of content under the heading "Nuclei, Particles, and Their Interaction" instead of "Solids." The editors of the Russian original apologize to the author and to the readers for this error.